Constraints on regional drivers of relative sea-level change around Cordova, Alaska

Ed Garrett[1]*, Natasha Barlow[1], Hannah Cool[1], Darrell Kaufman[2], Ian Shennan[1], Paul Zander[2]

Affiliations

[1] Sea Level Research Unit, Department of Geography, Durham University, Durham, DH1 3LE, UK

[2] School of Earth Sciences and Environmental Sustainability, Northern Arizona University, Flagstaff, AZ 86011-4099, USA

* Corresponding author. Now at The Geological Survey of Belgium, Royal Belgian Institute for Natural Sciences, Jennerstraat 13, 1000 Brussels, Belgium. Email: egarrett@naturalsciences.be

Key words: Relative sea level, Little Ice Age, 1964 Alaskan earthquake, isolation basin, diatom

ABSTRACT

New records of paleoenvironmental change from two lakes near Cordova, south central Alaska, combined with analysis of previously reported sediment sequences from the adjacent Copper River Delta, provide quantitative constraints on a range of Earth system processes through their expression in relative sea-level change. Basal sediment ages from Upper Whitshed Lake indicate ice-free conditions by at least 14,140 – 15,040 cal yr BP. While Upper and Lower Whitshed Lakes provide only upper limits to relative sea-level change, interbedded layers of freshwater peat and intertidal silt extending more than 11 m below present sea level in Copper River Delta indicate net submergence over the last 6000 years and multiple earthquake deformation cycles. In contrast, Lower Whitshed Lake, situated just above present high tide level, records only one episode of marine sedimentation, commencing AD 1120 – 1500, that we interpret as the result of isostatic subsidence due to Little Ice Age mass accumulation of the Chugach Mountain glaciers. Lower Whitshed Lake also records isostatic uplift at the end of the Little Ice Age before the end of marine sedimentation caused by ~1.5 m coseismic uplift in the great Alaska earthquake of AD 1964.

We successfully explain the records of relative sea-level change from both Copper River Delta and the Whitshed Lakes by integrating the effects of eustatic sea-level rise, glacial isostasy, earthquake deformation cycles, sediment loading, sediment compaction and late Holocene changes in glacier mass into a single model. This approach provides initial quantitative constraints on the individual contributions of these processes. Taking reasonable estimates of eustasy, post-Last Glacial Maximum and Neoglacial glacial isostatic adjustment and a simple earthquake deformation cycle, we demonstrate that sediment loading and sediment compaction are both contributors to relative sea-level rise at Copper River Delta, together producing subsidence averaging approximately 1.2 mm yr^{-1} over the mid to late Holocene. Further isolation basin studies have the potential to greatly improve our understanding of the individual contributions of these processes in this highly dynamic region.

1. Introduction

On many timescales, from greater than the Quaternary to sub-annual, the coastal environment of south central Alaska is highly dynamic, resulting from the interactions between climate change, ice sheet history, tectonics, erosion, mountain-building and relative sea-level change. Rapid exhumation, erosion through multiple glacial cycles, tectonics and fault alignments interact over million-year timeframes (e.g. Enkelmann et al., 2008); ice streams that reached the edge of the continental shelf at the Last Glacial Maximum, ~22-20,000 yr BP (Molnia and Post, 1995), had retreated to inland of the present coast, and in some cases well inside their present extent by ~15,000 yr BP (Pasch et al., 2010); the sediment load of the Copper River, ~70 – 140 x 10^6 tons yr^{-1}, is one of the 20 largest in the world (Jaeger et al., 1998; Milliman and Syvistski, 1992); and sediment sequences in the Copper River Delta provide one of the best archives of megathrust earthquakes, ten in the past 6000 years (Carver and Plafker, 2008), including the Mw 9.2 earthquake of March 1964. Lateral variations in lithospheric and upper mantle properties in this plate boundary location mean that the parameters of global glacial isostatic adjustment (GIA) models may give poor estimates of millennial-scale changes in relative sea level (RSL) and shorter term glacier fluctuations during the Little Ice Age may dominate present patterns of vertical land deformation (James et al., 2009a, b; Larsen et al., 2005; Sauber et al., 2000).

In this paper we use contrasting lacustrine and tidal marsh sediment sequences to provide quantitative constraints on the local timing of deglaciation, relative sea-level change and the contributions of processes that can lead to spatial and temporal differences in land surface uplift and subsidence. We present new data from sediment cores taken from two lakes at Point Whitshed, near Cordova (Figure 1) and contrast the record of sea-level change with that from Copper River Delta, 30-40 km to the east. We conclude with a model to demonstrate the interactions of processes that contribute to land surface deformation and relative sea-level change.

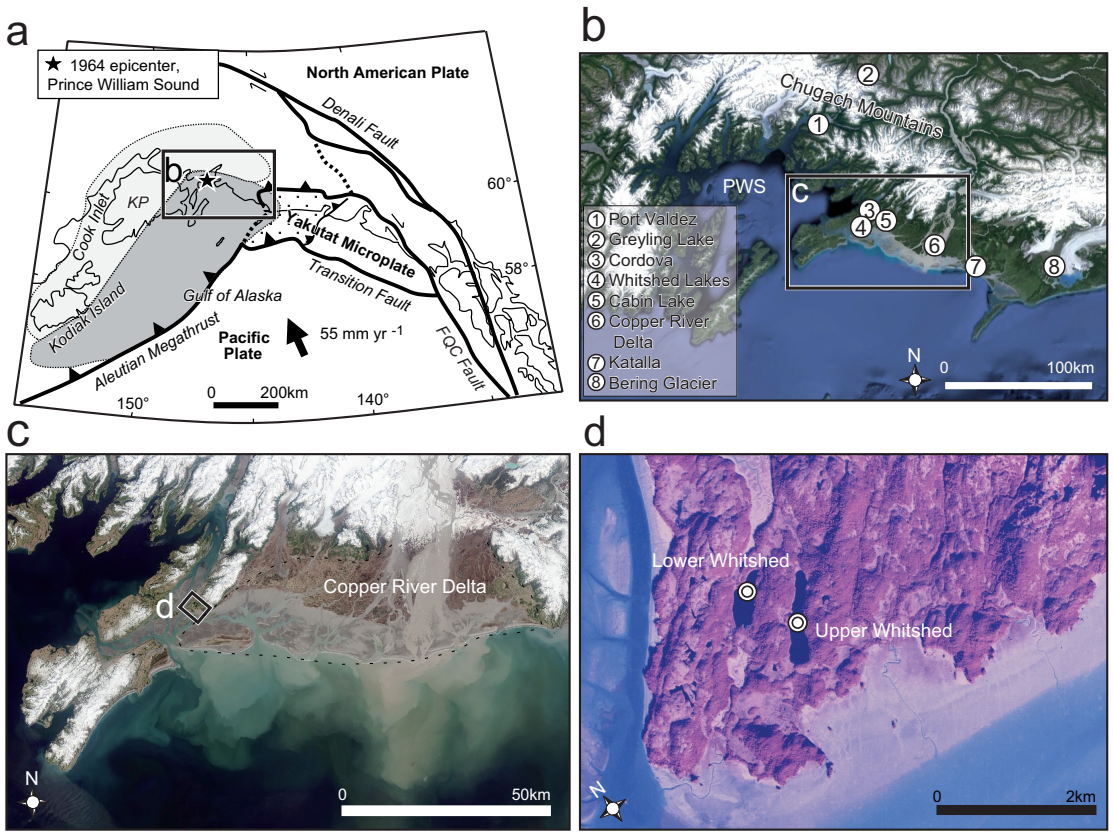

Figure 1: Tectonic setting of south central Alaska. (a) Approximate area of coseismic subsidence (light grey) and uplift (dark grey) in 1964. KP: Kenai Peninsula, FQC Fault: Fairweather – Queen Charlotte Fault. (b) Google Earth image of Prince William Sound (PWS) with the location of sites discussed. (c) Landsat image of sediment plumes emanating from the Copper River (data available from NASA Earth Observatory). The dashed black line delineates the approximate subaerial extent of the delta. (d) AD 1971 aerial photograph of Point Whitshed (data available from U.S. Geological Survey Earth Explorer), including the coring locations in Upper and Lower Whitshed Lakes.

2. Study area

2.1 Tectonic setting

Point Whitshed lies towards the eastern limit of the Alaska-Aleutian megathrust (Figure 1). Here, the subducting Yakutat microplate underthrusts the North American plate and is itself underthrust by the Pacific plate (Freymueller et al., 2008; Fuis et al., 2008), which moves approximately northward at ~55 mm yr^{-1}. Large to great (Mw > 8) earthquakes on any part of the active interfaces may result in sudden surface deformation. The 1964 earthquake ruptured the Prince William Sound and Kodiak segments of the Alaska-Aleutian megathrust, producing surface deformation over 170,000-200,000 km^2 of south central Alaska (Plafker, 1969). A broad zone of uplift affected the coastline of the Gulf of Alaska and eastern Prince William Sound (Figure 1). Plafker (1969) estimates coseismic uplift at Point Whitshed of 1.7 m, from raised barnacles, and ~1.9 m at the Cordova tide gauge, ~13 km to the northeast. Paleoseismic investigations record ten great earthquakes in the last 5000 years at sites in the Copper River Delta (Carver and Plafker, 2008; Plafker et al., 1992; Shennan et al., 2014), a likely consequence of rupturing of one or more segments of the Alaska-Aleutian megathrust (Shennan et al., 2009).

2.2 Glacial history

Ice fields and mountain glaciers currently cover approximately 74,700 km^2 of Alaska (Kaufman and Manley, 2004). During the Last Glacial Maximum, the western extension of the North American Cordilleran Ice Sheet covered south central Alaska, with ice covering 727,800 km^2, including areas of the continental shelf (Hamilton and Thorson, 1983; Kaufman and Manley, 2004; Molnia and Post, 1995). The region was largely deglaciated by some time prior to approximately 14-12,000 cal yr BP (Huesser, 1960; Kaufman and Manley, 2004; Mann and Hamilton, 1995; Sirkin and Tuthill, 1987). By the start of the Holocene, ice margins were at or behind their modern positions (Barclay et al., 2009). Neoglacial advances occurred between ~3300-2900 yr BP, and again during the first millennium AD, with the main interval in the Chugach and Kenai Mountains c. AD 430-720 (Barclay et al., 2009; 2013; Calkin et al., 2001; Reyes et al., 2006; Wiles et al., 2008; Wiles and Calkin, 1994). During the Medieval Warm Period (~AD 900-1240), glaciers receded and forests regenerated in the forefields of many glaciers (Barclay et al., 2009). Late Holocene glacial advance culminated in

the second millennium AD during the Little Ice Age (LIA), with early advances underway in Alaska from AD 1180-1330. The middle and late advances (c. AD 1540-1720 and AD 1810-1890 respectively) resulted in Holocene maxima for many land-terminating glaciers in the Chugach Mountains (Barclay et al., 2009; 2013; Calkin et al., 2001; Molnia, 2008; Wiles et al., 1999; 2008; Wiles and Calkin, 1994). The majority of Alaskan mountain glaciers have retreated and thinned from their maximum LIA positions. Estimates of late 20th century contributions to sea-level rise from the melting of Alaskan glaciers range from 0.04 ± 0.01 mm yr^{-1} to 0.14 ± 0.04 mm yr^{-1} (Arendt et al., 2002; Berthier et al., 2010; Larsen et al., 2007).

2.3 Site selection

Two lakes, Upper and Lower Whitshed, lie close to Point Whitshed, approximately 13 km southwest of Cordova (Figure 1). The basins are sufficiently deep (>5 m) to prevent stratigraphic disturbance by freezing to the lake floor, yet small enough for their salinity to rapidly respond to changes in sea level. USGS topographic maps show Upper Whitshed Lake just below the 100 ft contour and maps held by the landowner place Lower Whitshed Lake within the 10 ft contour (Eyak Native Corporation, pers. comm., 2011). Lower Whitshed Lake is not currently inundated by even the highest tides (Highest Astronomical Tide (HAT) = 2.87 m above Mean Sea Level (MSL)) and we estimate the elevation of the sill of the basin as 4 ± 1 m MSL. We estimate the Upper Whitshed Lake sill as 33 ± 2 m MSL.

3. Methods

3.1 Lakes as isolation basins

We employ an isolation basin approach, investigating sediments contained within natural topographic depressions that reflect phases of connection to or separation from the sea. This approach, developed along Scandinavian coastlines (e.g. Hafsten and Tallantire, 1978; Krzywinski and Stabell, 1984; Svendsen and Mangerud, 1987), provides reconstructions of late Quaternary relative sea-level change in Scotland (Shennan et al., 1994; 1995), Iceland (Lloyd et al., 2009; Rundgren et al., 1997), Canada (Hutchinson et al., 2004; James, 2005; 2009a; Josenhans et al. 1995) and Antarctica (Bentley et al., 2005; Zwartz et al., 1998). Long et al. (2011) provide a comprehensive review of the approach, with reference to Holocene relative sea-level reconstructions for Greenland. The type of sediment accumulating in an

isolation basin reflects the position of the basin relative to sea level (Figure 2a). Basins above tidal influence, approximately HAT, will accumulate freshwater sediments while basins with a sill elevation within or below the intertidal zone will accumulate brackish and marine sediments respectively. As relative sea-level change moves a basin from one of these positions to another, the type of sediment accumulating changes accordingly (Figure 2b, c). Identifying and dating contacts between sedimentary units constrains the timing of ingression or isolation.

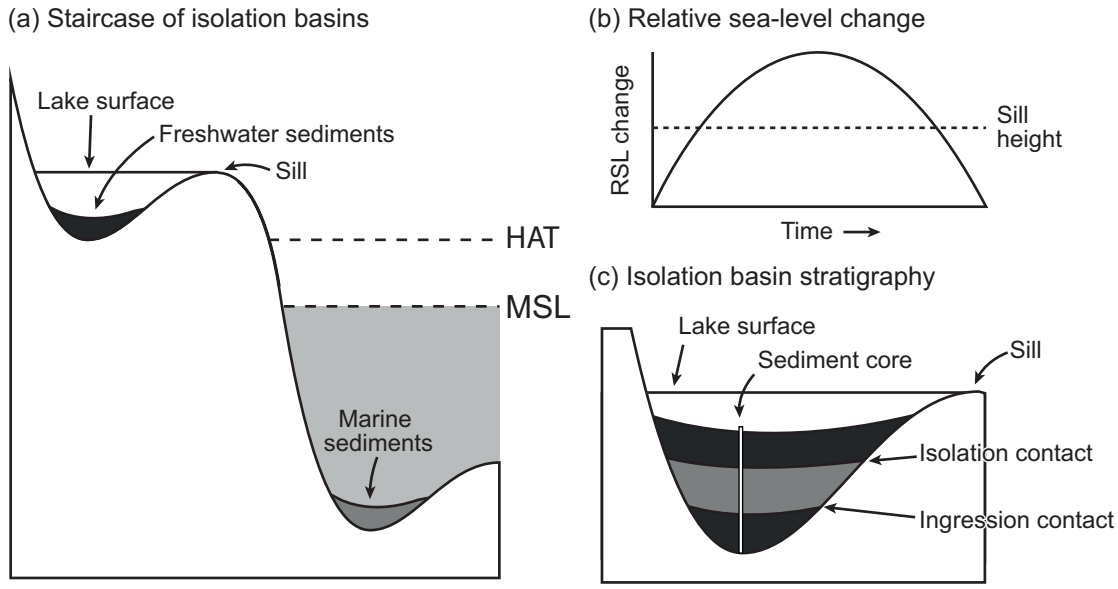

Figure 2: (a) Staircase of two isolation basins at elevations above and below sea level, accumulating freshwater and marine sediments respectively. Note that the higher basin is only freshwater if the sill is above the influence of tides at all stages of the tidal cycle. (b) Hypothetical relative sea-level curve leading to (c) an isolation basin containing a stratigraphic record of ingression followed by isolation.

We investigate two potential isolation basins located above present mean sea level. Cores from Lower Whitshed Lake were retrieved in March 2010 from the frozen surface of the lake using a percussion corer and a gravity surface corer at a single site (60.472°N, 145.922°W; Figure 1). We recovered a 165 cm surface core (10-WS-1A), with an intact sediment-water interface, and a 262 cm percussion core (10-WS-2). The sedimentary sequences of 10-WS-1A and 10-WS-2 have been spliced based on visual colour changes and magnetic susceptibility data. Comparison of the cores indicates core 10-WS-2 is missing the uppermost 3.5 cm of sediment and continues to 265.5 cm below lake floor (BLF).

Cores were retrieved from Upper Whitshed Lake in June 2011 using a percussion corer and a gravity surface corer from a floating platform. This paper discusses cores from a site at 60.466°N, 145.919°W (Figure 1), which contains a longer record than other cored sub-basins. The 427 cm percussion core from this site (11-UW-2) extends to 442 cm BLF, while the surface core (11-UW-2A) measures 46 cm.

3.2 Biostratigraphy

Past isolation basin environments are reconstructed using diatom analysis. Diatoms, silica-rich unicellular algae, live in aquatic environments and display restricted niches controlled by environmental factors. Distinct assemblages of species are found in freshwater, brackish and marine environments (Vos and de Wolf, 1993). Preparation of diatom samples follows standard procedures (Palmer and Abbott, 1986). Species identification follows Hartley et al. (1996), Hemphill-Haley (1993), Patrick and Reimer (1966, 1975) and van der Werff and Huls (1958-1974), with the results plotted in C2 (Juggins, 2003) and species classified into five categories of salt tolerance (Hemphill-Haley, 1993). Changes in the relative abundance of diatoms in different salinity classes provide qualitative indications of changes in marine influence.

3.2 Chronology

A radionuclide approach constrains the upper part of the age model from Lower Whitshed Lake. We use the Plutonium (Pu) activity profile to locate the AD 1953 onset of nuclear weapons testing and the 1963 peak fallout (Ketterer et al., 2004). The profile was analysed using an inductively coupled plasma mass spectrometer (ICP-MS) at Northern Arizona University.

AMS radiocarbon dating constrains the age model for Upper Whitshed Lake and the lower part of Lower Whitshed Lake. Wet sieving of 0.5- to 2-cm-thick sediment samples provided macrofossils for ^{14}C dating, with analysis undertaken at the Keck Carbon Cycle AMS Facility at UC Irvine. Dates are calibrated to years prior to 1950 AD (cal yr BP) using OxCal 4.2 (Bronk Ramsey, 2009) and the IntCal13 calibration curve (Reimer et al., 2013).

We construct age-depth models for both lakes using the program Bacon 2.2 in R (Blaauw and Christen, 2011), incorporating the radiocarbon (Table 1) and artificial radionuclide fallout data. Bacon uses a Bayesian approach to construct age-depth relations through the calibrated-age probability distributions of radiocarbon dates, or other age information. The sedimentary sequence is divided into discrete segments; most importantly, the routine allows the inclusion of stratigraphic information, such that shifts in sedimentation rate are aligned with stratigraphic boundaries. Millions of Markov Chain Monte Carlo iterations are run and the average of these provides the best fit model. Confidence intervals are calculated as the 2σ range of the iterations. We refer to basal radiocarbon dates in calibrated years before present (cal yr BP), with present = 1950 AD, and all other ages in years AD.

Table 1: Radiocarbon dates from the Whitshed Lakes sediment cores.

Lab ID (UCIAMS)	Core ID	Bottom Depth BLF (cm)	^{14}C Age (yr BP ± 1σ)	Calibrated Age (cal yr BP, 2σ)	Material
Lower Whitshed Lake (60.472°N, 145.924°W)					
76307	10-WS-2	49.0	135±20	10 - 270	*Tsuga* needle fragments, bryophyte capsules
82286	10-WS-2	98.5	175±20	0 - 290	*Tsuga* needles, alder leaf fragments, conifer seed, wood fragments
76308	10-WS-2	110.0	455±15	500 - 520	*Picea* needles and twigs, *Tsuga* needle
82287	10-WS-2	133.5	1970±15	1880 - 1970	Two *Picea* and one *Tsuga* needle, conifer seed wing, conifer seed fragment
82288	10-WS-2	150.5	2875±20	2930 - 3070	Conifer wing fragment, *Piceae* seed and needles, chitin from aquatic insects
82289	10-WS-2	170.5	3960±30	4300 - 4520	All aquatic material, caddis fly case
82290	10-WS-2	195.5	5130±20	5760 - 5930	All aquatic chitin
82291	10-WS-2	204.5	5635±20	6320 - 6480	*Cladocera* chitin, terrestrial leaf vein, *Alnus* leaf, moss fragments
82292	10-WS-2	224.5	7525±20	8330 - 8390	All aquatic; chitin, Chironomid head fragments, non-specific plants (moss branches?)
76309	10-WS-2	254.5	9355±25	10510 - 10660	Unspecified leaf fragments
82293	10-WS-2	266.5	8875±30	9830 - 10180	Terrestrial leaf fragments, aquatic chitin, *Najas* (floating leaf aquatic plant)
Upper Whitshed Lake (60.466°N, 145.920°W)					
100081	11-UW-2-3	363.0	9530±60	10610 - 11110	Leaf fragments and bryophyte twigs
104764	11-UW-2-3	396.5	11070±40	12810 - 13060	Terrestrial leaf fragments (from small shrub), lots of bryophyte twigs
100082	11-UW-2-3	435.0	12430±100	14140 - 15040	Bryophyte, unidentifiable fragments, *Ericacae* seed, leaf fragments

3.3 GIA modelling

Following Barlow et al. (2012), we use a regional glacial isostatic adjustment (GIA) model to infer a history of late Holocene land-level change driven by changes in the mass of the regional ice load. A simple postglacial rebound calculator, TABOO (Spada, 2003; Spada et al., 2003, 2004), models the spatial pattern and magnitude of solid Earth displacement during and following the LIA in south central Alaska. TABOO uses a layered, non-rotating, incompressible, self-gravitating, Maxwell viscoelastic, spherically symmetric Earth model in which the density, shear modulus and viscosity of each layer is constant. We use the Larsen et al. (2004; 2005) 'Neoglacial' ice-load model, which distributes changes in ice volume over 531 spherical symmetrical 20-km-diameter disks to estimate ice thickness changes for the last 2000 years. The model includes an early advance from AD 500-700 followed by a three-phase advance from AD 1250 to the LIA maximum in AD 1900. The spherical harmonics of the GIA model are expanded to degree and order 1024 to allow the model to be sensitive to the small load at 60°N. Seismic observations from subduction margins identify the presence of an asthenosphere between the lithosphere and upper mantle, with the lithosphere–asthenosphere boundary being fundamental in allowing plate movement (Anderson, 1975). Barlow et al.'s (2012) earth model includes an asthenosphere to 220 km that has model viscosity an order of magnitude lower than the underlying mantle. The asthenospheric thickness is therefore 220 km minus the modelled lithospheric thickness. The mantle is modelled as a homogenous layer with a viscosity of 4×10^{20} Pa s. Table 2 provides the rheology of the 'accepted' earth models from Barlow et al. (2012), which we use to provide RSL outputs for the Cordova area. We note that Barlow et al.'s (2012) rejection of two earth models with low lithospheric thickness and low asthenospheric viscosity is based upon GPS data from the interseismically uplifting Cook Inlet rather than the subsiding eastern Prince William Sound; however, given the current absence of other data to constrain the rheology, we believe Barlow et al.'s (2012) accepted models are still currently the best fit solutions for south central Alaska.

Table 2: Rheology of 'accepted' Earth models from Barlow *et al*. (2012). The modelled asthenosphere extends to 220 km depth and the mantle viscosity underlying the asthenosphere is 4 x 10^{20} Pa s in all instances.

Model number (Figure 6)	Lithospheric thickness (km)	Asthenosphere viscosity (x 10^{19} Pa s)
1	110	4.0
2	110	0.8
3	110	0.4
4	110	0.1
5	60	4.0
6	60	0.8

4. Results

4.1 Lower Whitshed Lake

We identify three distinct lithologic units from the Lower Whitshed Lake gravity and percussion cores (Figure 3a). Sediments from the base of the core at 265.5 to 103.5 cm BLF consist of brown gyttja. A diffuse boundary marks a transition to grey silt with occasional plant macrofossils, which continues from 103.5 to 4 cm BLF. At this depth, an abrupt contact divides the silt from an overlying 4-cm-thick layer of brown gyttja.

The age model for the sedimentary sequence includes the age of the top of core 10-WS-1A (2010), the onset and peak of nuclear weapons testing as recorded in the Pu activity profile from core 10-WS-1A and 11 radiocarbon dates from core 10-WS-2 (Table 1, Figure 3a, supplementary Table S1). The model indicates a basal age of 9810 – 11,680 cal yr BP.

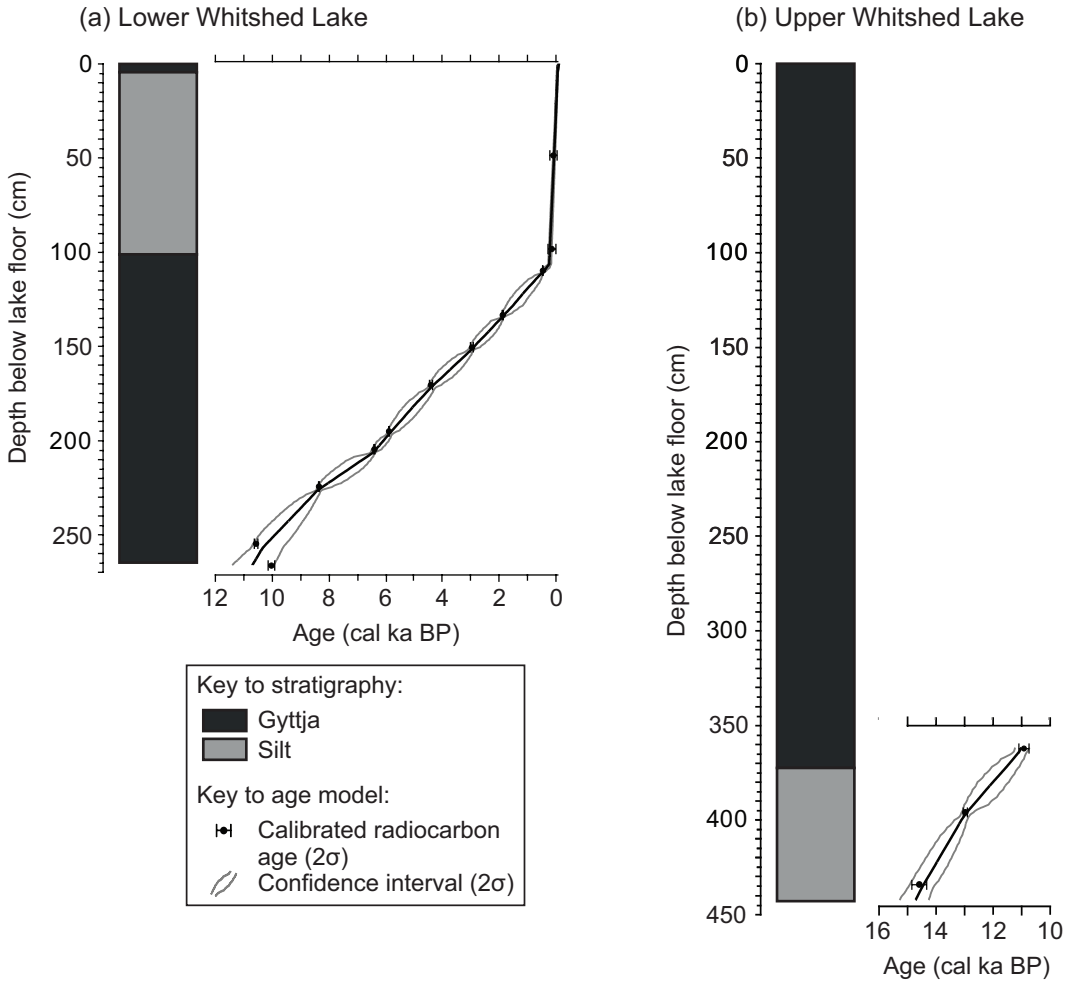

Figure 3: Stratigraphy and age-depth models for (a) Lower Whitshed Lake and (b) Upper Whitshed Lake created using Bacon in R (Blaauw and Christen, 2011). Radiocarbon data are listed in table 1.

Diatom assemblages from the base of core 10-WS-2 are dominated by salt intolerant freshwater species including *Tabellaria fenestrata* and *Cyclotella antiqua* (Figure 4). We find assemblages containing predominantly freshwater diatom species in all samples below 112.5 cm BLF. Above 112.5 cm BLF we observe the appearance of marine species, which increase in abundance and contribute approximately 40 % of the assemblage by the upper contact of the gyttja at 103.5 cm BLF. The age model places the introduction of marine species to AD 1120 – 1500 and the gyttja – silt contact to AD 1620 – 1700.

Diatom assemblages from the silt layer in core 10-WS-2 include marine species, including *Diploneis fusca* and *Gyrosigma wansbeckii*, and brackish species, including *Nitzschia sigma* (Figure 4). Freshwater species decline to less than 30 % of the total assemblage by 100.5 cm BLF, equivalent to a modelled age of AD 1630 – 1710. Marine diatoms increase in

abundance, reaching 80 % of the assemblage in some samples, before declining to below 50 % around 33.5 cm BLF, corresponding to AD 1850 – 1910.

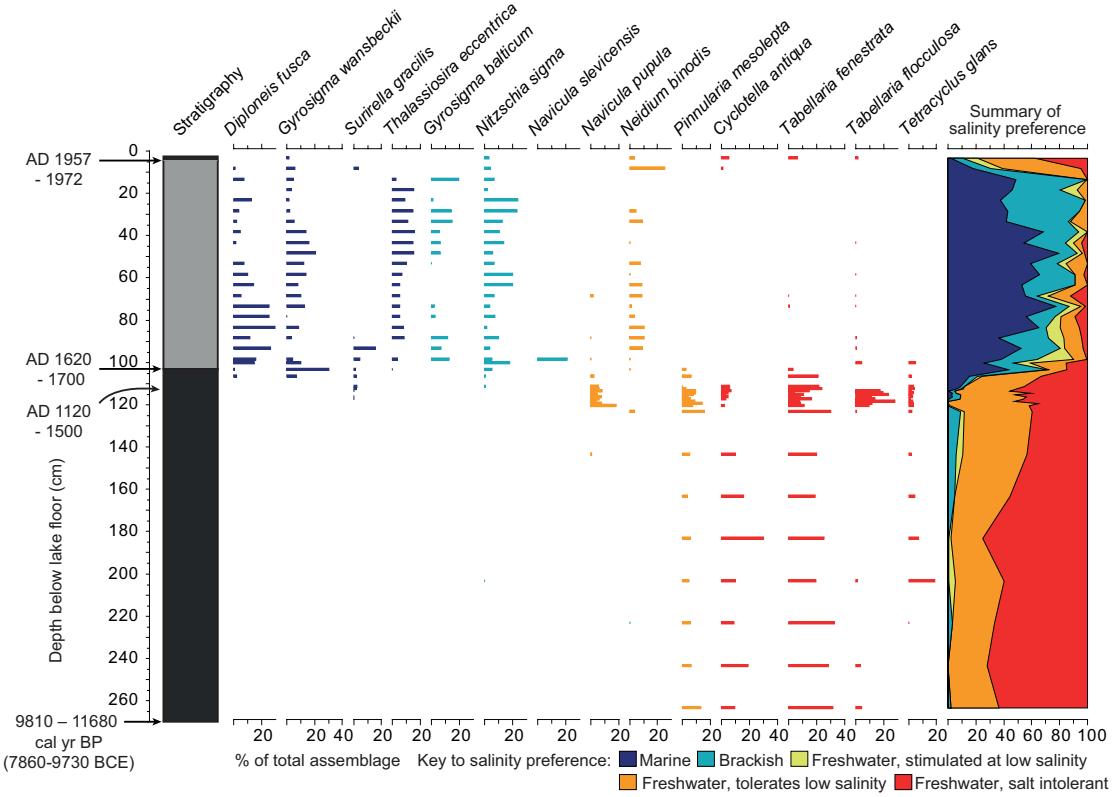

Figure 4: Summary of diatom assemblages for Lower Whitshed core 10-WS-2, showing species exceeding 15% in one or more sample. Arrows indicate modelled calibrated ages derived from the age model in Figure 3. Key to stratigraphy displayed in Figure 3.

Further increases in freshwater species that can only tolerate low salinities occur before the abrupt transition from silt to gyttja at 4 cm BLF. We find a freshwater diatom assemblage in the surficial gyttja layer in core 10-WS-2 (Figure 4). We infer the timing of the gyttja – silt contact through comparison with Pu activities in the surface core 10-WS-1A (Figure 5). Plutonium is first detected at 9.5 cm BLF and the activity per kilogramme peaks at 1.7 cm. The high sedimentation rate in the silt layer, inferred from the radiocarbon data, results in lower Pu activity than in the more slowly accumulating gyttja. To account for this, we multiply the Pu activity by the sedimentation rate to estimate the rate of Pu supply (Figure 5). The age model, incorporating peak Pu fallout (AD 1963) at 4.5 cm, constrains the timing of the silt – gyttja contact to AD 1957 – 1972.

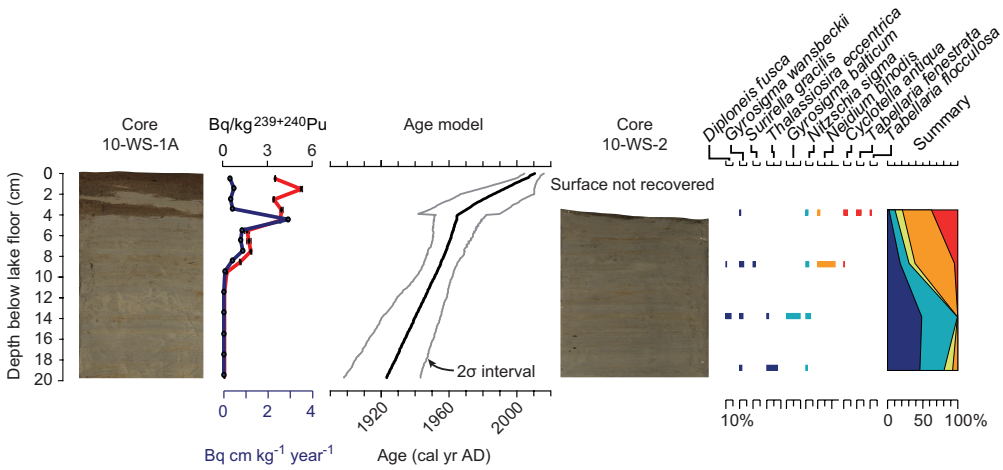

Figure 5: Comparison of Plutonium activity profiles and the age model from the top 20 cm of Lower Whitshed core 10-WS-1A with diatom assemblage data from core 10-WS-2. To account for higher sedimentation rates in the silt layer than in the gyttja, we multiply the Pu specific activity profile (red line) by the sedimentation rate to estimate the rate of Pu supply (blue line). Key to diatom salinity preference displayed in Figure 4.

4.2 Upper Whitshed Lake

The Upper Whitshed Lake cores contain two lithologic units: grey silt with occasional terrestrial plant macrofossil fragments from 442 to 372 cm BLF and brown gyttja from 372 cm to the sediment – water interface. The age model for the lowest 1 m of the core (the focus of this study) is based on three radiocarbon dates from the silt layer and the base of the gyttja (Table 1, Figure 3b). A radiocarbon date from 434 – 435 cm BLF provides a minimum age for the onset of sediment accumulation in Upper Whitshed Lake of 14,140 – 15,040 cal yr BP. Extrapolation to the base of the core at 442 cm BLF using the age model provides a marginally older age of 14,170 – 15,220 cal yr BP (Figure 3b).

We examine diatom assemblages from the basal silt in core 11-UW-2 to determine whether it is of marine or freshwater origin. Samples from throughout the silt layer contain diatom assemblages that include the freshwater, salt intolerant species *Tabellaria flocculosa*, *T. fenestrata* and *Pinnularia subcapitata*, alongside freshwater species capable of tolerating low salinities, including *Pseudostaurosira brevistriata*, *Fragilaria construens* var. *venter* and *Staurosirella pinnata* (for full species list see supplementary Table S2).

5. Discussion

5.1 Timing of deglaciation

The radiocarbon date of 14,140 – 15,040 cal yr BP at the base of the Upper Whitshed Lake sequence provides a minimum date for deglaciation from this low elevation site, with freshwater sediments starting to accumulate following local ice retreat from the Late Wisconsin ice extent. The date fits with a regional chronology of retreat of ice in the south central Chugach Mountains and ice free conditions in Prince William Sound from ~14,000 cal yr BP (Kaufman and Manley, 2004; Mann and Hamilton, 1995) and a similar age for Bering Glacier (Pasch et al., 2008). A date at the base of a lacustrine sequence near Port Valdez, Prince William Sound, indicates ice free conditions from before 12,000 cal yr BP (Reger, 1991). Similarly, ice had retreated from the lower part of the Copper River Delta prior to 14,000 cal yr BP (Huesser, 1960; Sirkin and Tuthill, 1987) and from Cabin Lake at the south of the Chugach Mountains by 11,300 cal yr BP (Zander et al., 2013). Dates from Greyling Lake suggest ice-free conditions above 1000 m elevation by 13,000 cal yr BP and perhaps as early as 15,000 cal yr BP in the central Chugach range (McKay and Kaufman, 2009). Further west, ice-free vegetated conditions occurred in Kenai Peninsula by 16,500 cal yr BP (Mann and Hamilton, 1995). In the Matanuska Valley, interior northern Chugach, deglaciation was underway prior to 13,200 cal yr BP (Yu et al., 2008). Our new radiocarbon data confirms that ice in the Prince William Sound region had retreated onto the current landmass by 14,000 cal yr BP.

5.2 The Whitshed record of relative sea-level change and great earthquakes

The absence of stratigraphic or diatom evidence for marine inundation into Upper Whitshed Lake implies that sea level has been below 30.13 ± 2 m since the site became ice free, no later than 14,140 – 15,040 cal yr BP. Freshwater diatom assemblages from the lowermost sampled sediments at Lower Whitshed Lake (Figure 4) indicate that relative sea level was below 1.13 ± 1 m at 9,810 – 11,680 cal yr BP (Table 3). These freshwater basal sediments provide only upper limits for relative sea level, which could have been at any level below the basins at the time.

Table 3: Relationships between lake elevations and the transition between fresh and brackish/marine sediments within a lake used to reconstruct relative sea-level change.

	Present elevation: m MSL	Indicative meaning of sediment contact: tidal level	Indicative meaning of sediment contact: m MSL	Relative sea level indicated by sediment contact in the basin: m
Upper Whitshed Lake	33 ± 2	HAT	2.87	30.13 ± 2
Lower Whitshed Lake	4 ± 1	HAT	2.87	1.13 ± 1

Sea-level curves from many formerly glaciated regions feature postglacial relative sea levels tens to hundreds of metres above present (e.g. Ingólfsson et al., 1995; Shennan et al., 1995; Svendsen and Mangerud, 1987), reflecting isostatic uplift following deglaciation. In the vicinity of Vancouver, Canada, relative sea level fell from 150 m to -15 m between 14,000 cal yr BP and 11,500 cal yr BP, reflecting rapid uplift resulting from the retreat of the Cordilleran Ice Sheet (Clague et al., 1982; Hutchinson et al., 2004). James et al. (2000) suggest the rapid rate of sea-level fall around Vancouver necessitates lower mantle viscosity values than for non-subduction zone settings. The retreat of the Cordilleran ice sheet from south central Alaska combined with low viscosity asthenosphere estimates (Barlow et al., 2012) may similarly imply very rapid postglacial land uplift at Point Whitshed.

The first direct evidence of relative sea-level change at Point Whitshed is the marine and brackish diatom assemblage in the Lower Whitshed Lake silt layer (103.5 – 4 cm BLF), which demonstrates connection to the sea. The occurrence of marine diatoms after AD 1120 – 1500 implies relative sea-level rise and the beginning of the ingression of tides into the basin (Figure 4). Sea-level rise and basin ingression continued until at least AD 1620 – 1700, with a transition to silt deposition indicating the dominance of marine over terrestrial sediment sources. The decline in marine species around AD 1850 – 1910 marks falling relative sea level and the beginning of the isolation of the basin from the sea. The abrupt silt – gyttja contact, the transition to freshwater diatom assemblages and the modelled age of AD 1957 – 1972 are all consistent with coseismic uplift in 1964 abruptly completing the isolation of the basin.

Observations and modelling of recent ice retreat and land uplift from a number of locations in south central and southeast Alaska (Larsen et al., 2005; Sauber et al., 2000) suggest that glacial isostatic responses to Little Ice Age and older Neoglacial changes in the mass of local

ice caps and glaciers can produce measurable changes in relative sea level. Our GIA modelling suggests the timing of ingression and isolation of Lower Whitshed Lake is consistent with relative sea-level rise and subsequent fall associated with isostatic depression during the Little Ice Age (Figure 6). The model predicts land-level change and change in the height of the geoid over the last 1000 years for the six earth models (Table 2) constrained by observations in south central Alaska (Barlow et al., 2012). We convert this to RSL over the last 1000 years by subtracting the land-level change from the ocean geoid height deformation (Figure 6). The differing earth model parameters result in a spread of model solutions, in particular for the first 400 years, due to the differing rheological structures, with the thickness and viscosity parameters of the asthenosphere being the primary controls on earth response to changes in ice load during this period. As a result, the model with the lowest viscosity (number 4) shows the greatest magnitude of RSL change during the last 1000 years.

The cumulative effect of increased ice mass during the Little Ice Age results in RSL rise as the land is isostatically depressed. The models predict RSL around Point Whitshed to be 0.5 to 1.5 m below present at AD 1100, rising above present at ~AD 1600. The timing of this rise is entirely consistent with marine diatoms suggesting ingression of Lower Whitshed Lake. Modelled RSL is then 0.2 to 0.6 m above present during the maximum Little Ice Age advance at AD 1900, after which it falls as ice begins to retreat at the start of the 20th century (Barclay et al., 2009; Calkin et al., 2001). The modelled RSL fall is rapid following unloading as the low viscosity of the modelled asthenosphere responds with rapid rebound.

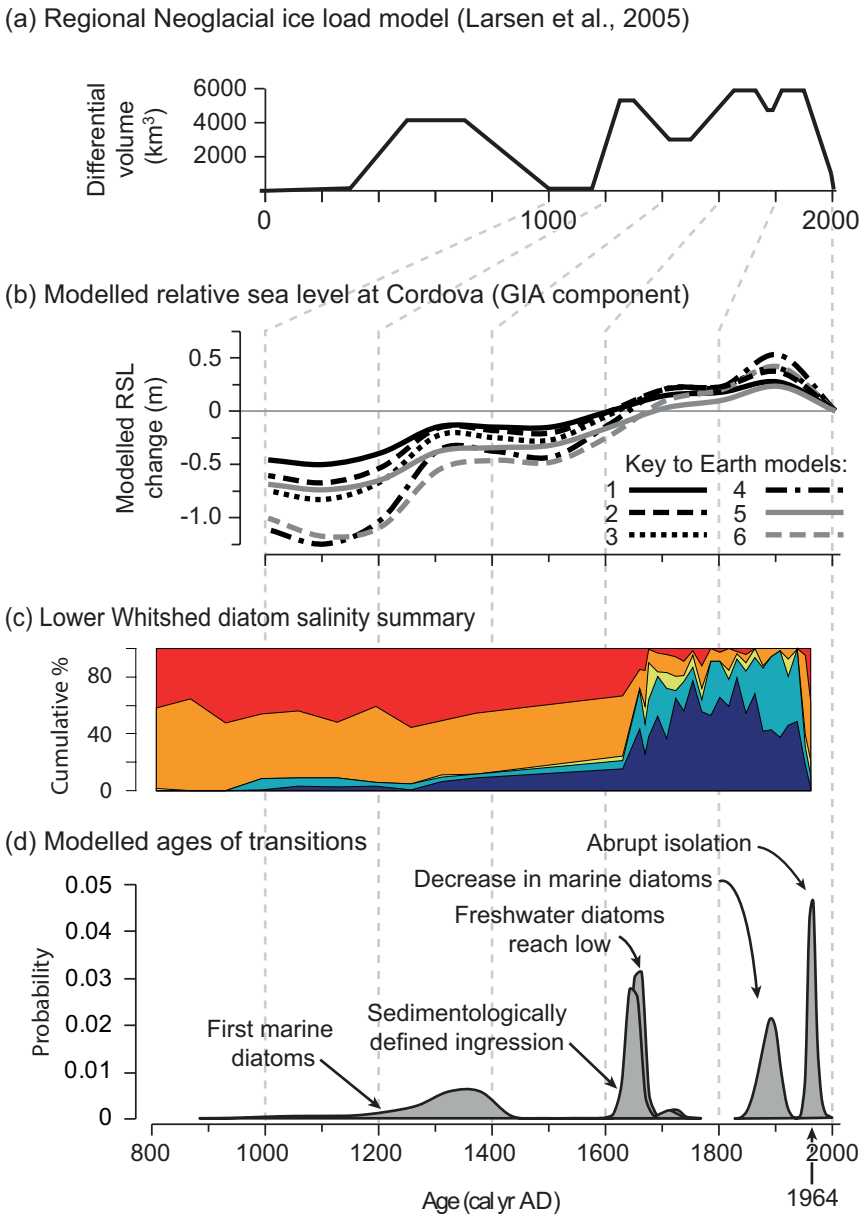

Figure 6: (a) The regional Neoglacial ice load model (Larsen et al., 2005) used in (b) to predict relative sea level at Cordova (glacial isostatic components only). We compare this with (c) the Lower Whitshed Lake diatom salinity summary and (d) modelled ages (probability distribution functions) of transitions in the Lower Whitshed core.

5.3 Integrating contributions to RSL change

In contrast to this record of just one period of ingression into the lower lake, to the east of Point Whitshed, peat horizons encountered more than 11 m below the lowest current elevation of peat formation imply net submergence in the Copper River Delta over the last 6000 years (Figure 7) and provide records of coseismic uplift and interseismic subsidence

over multiple earthquake deformation cycles (Carver and Plafker, 2008; Plafker et al., 1992). The absence of lithologic and biostratigraphic evidence of multiple earthquake deformation cycles at the low-lying Lower Whitshed Lake and the presence of evidence below sea level at Copper River Delta place important constraints on the contributions of different processes that control sea-level change and land surface vertical motions. In this section, we integrate the contributions of different processes that contribute to relative sea-level change at Whitshed Point and Copper River Delta.

GIA from the Last Glacial Maximum

We have no precise constraints on RSL other than deglacial ages that provide maximum constraints, until the earliest ages from Copper River Delta, which are from more than 11 m below present high tide (Figure 7). RSL constraints from other places to the east, such as Katalla (Shennan et al., 2014) and the Bering Glacier foreland (Shennan, 2009), may include the influence of upper plate faults (Chapman et al., 2011). In line with other plate boundary locations, we take a model of the GIA contribution from the melting of the Cordilleran Ice Sheet from the Last Glacial Maximum to be minimal or zero by 6000 cal yr BP (Figure 7). The predicted sea-level curve from this model (RSL_1) lies well above the observations from Copper River Delta, though below the maximum constraint from Point Whitshed. This approach assumes no effect from the collapse of a forebulge around the much larger of Laurentide Ice Sheet. Quantitative models of such forebulge effects (e.g. Argus and Peltier, 2010) remove data from plate boundary observations in their model development, as the likely Earth model parameters are very different to plate interiors. Therefore, while we may anticipate a contribution from forebulge collapse, producing essentially the same rate of subsidence at Copper River Delta and Whitshed lakes, we have found no published quantitative estimates and treat it as zero in our first analysis.

Multiple earthquake deformation cycles

We add an earthquake cycle influence to our model, basing the intervals on observations of regional patterns (Carver and Plafker, 2008; Shennan et al., 2014), assuming ~1.5m coseismic uplift, as in 1964 (Plafker, 1969), ~30% recovery since then and no net tectonic motion over multiple cycles (RSL_2 in Figure 8).

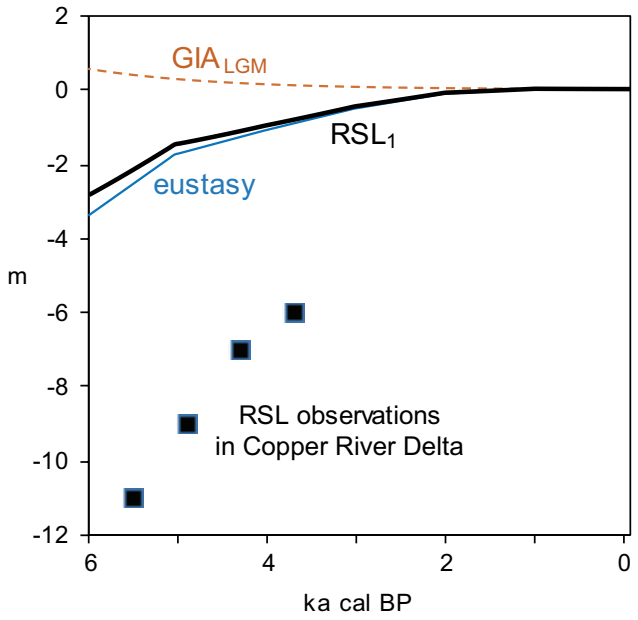

Figure 7: GIA-induced sea-level fall following the Last Glacial Maximum (GIA_{LGM}) and eustatic sea-level rise contribute to a first approximation of relative sea-level change (RSL_1), which does not fit observations from Copper River Delta (Plafker et al., 1992). Observations from isolation basins constrain sea level at Point Whitshed to elevations below 1.13 m ± 1 m from 9,810 – 11,680 cal yr BP until a single period of inundation within the last 1000 years.

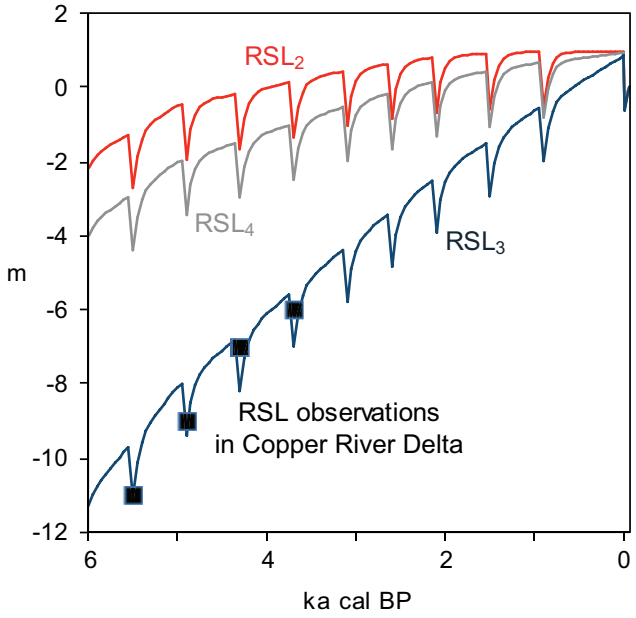

Figure 8: An earthquake deformation cycle is added to RSL_1 (Figure 7), assuming coseismic uplift of 1.5 m and no net tectonic motion over multiple cycles, to derive RSL_2. We require a combined influence of sediment loading and compaction of ~1.5 mm yr^{-1} to fit RSL observations from Copper River Delta (RSL_3). If subsidence at Copper River Delta relates entirely to compaction, relative sea-level change at Point Whitshed would lie on the red line (RSL_2). We reject this model as Lower Whitshed Lake does not record multiple ingressions across the sill. We derive RSL_4 by adding loading-induced subsidence of 0.3 mm yr^{-1} to RSL_2.

Sediment loading and sediment compaction

Geological observations from Copper River Delta are from peat layers within thick sequences of unconsolidated sediments. High contemporary sediment input from Copper River, 70 – 140 x 10^6 tons yr^{-1} (Jaeger et al., 1998; Milliman and Syvistski, 1992), and Holocene accumulations greater than 300 m in thickness (Carlson and Molnia, 1975) indicate two possible contributions to relative sea-level change: sediment loading on the crust and sediment compaction. We envisage these two processes as having different spatial expressions. Sediment compaction will be more localised, for example dependent upon sediment characteristics within the delta, whereas the sediment load will produce an isostatic contribution across the broader region, in the same way an increase in ice mass would. To produce a reasonable fit to the observations from the delta, we require a combined influence from loading and compaction of ~1.5 mm yr^{-1} to be added to RSL_2 (RSL_3 in Figure 8).

Different combinations of process-responses between sites

With the Whitshed lakes situated on bedrock and the Copper River Delta data from thick, unconsolidated sediment sequences, we may expect some additional subsidence at the latter, caused by sediment compaction. If the subsidence relates entirely to compaction, then relative sea-level change at Point Whitshed would lie on the red line in Figure 8 (RSL_2); if subsidence relates entirely to sediment loading, RSL at Point Whitshed would lie on the black line (RSL_3). As noted above, forebulge collapse, currently taken as zero, could be a contributor to subsidence at both sites.

With subsidence relating entirely to compaction, RSL_2 suggests multiple ingressions into Lower Whitshed Lake to approximately the same elevation as the most recent ingression, with each terminated by abrupt coseismic uplift. We reject this curve on two lines of evidence: first, there is only evidence for one period of marine ingression; second, the diatoms show a trend of RSL rise at the start, levelling off to a maximum, and a period of gradual fall before isolation in 1964. Therefore, we attempt to refine the model by partitioning the contributions from sediment loading and compaction. To obtain an initial estimate of the relative contributions of these factors, we run TABOO separately with a single disc to represent the solid Earth response to the Copper River Delta sediment load (Figure 9). Two model runs reflect total annual sediment accumulation rates of 70 and 140 x 10^6 t yr^{-1} (following Jaeger et al., 1998; Milliman and Syvistski, 1992). The smaller load

suggests subsidence at Point Whitshed and Copper River Delta at rates of 0.30 mm yr^{-1} and 0.47 mm yr^{-1} respectively. We add subsidence of 0.3 mm yr^{-1} to RSL_2 in Figure 8 to derive RSL_4. The larger annual sediment load suggests subsidence rates twice as large. These figures are of the same order of magnitude as estimates of subsidence due to sediment loading at the Mississippi Delta (Yu et al., 2012). The additional 0.6 – 1.0 mm yr^{-1} subsidence required to match the Copper River Delta observations (RSL_3) is in line with estimates of estuarine sediment compaction rates from the UK (Horton and Shennan, 2009) and substantially less than millennial-scale compaction rates of 5 mm yr^{-1} inferred from the Mississippi Delta (Törnqvist et al., 2008). With a more detailed ground survey of the elevation of the sill than currently available, we could further refine our estimates of the relative contributions of sediment loading and sediment compaction through the age of the ingression.

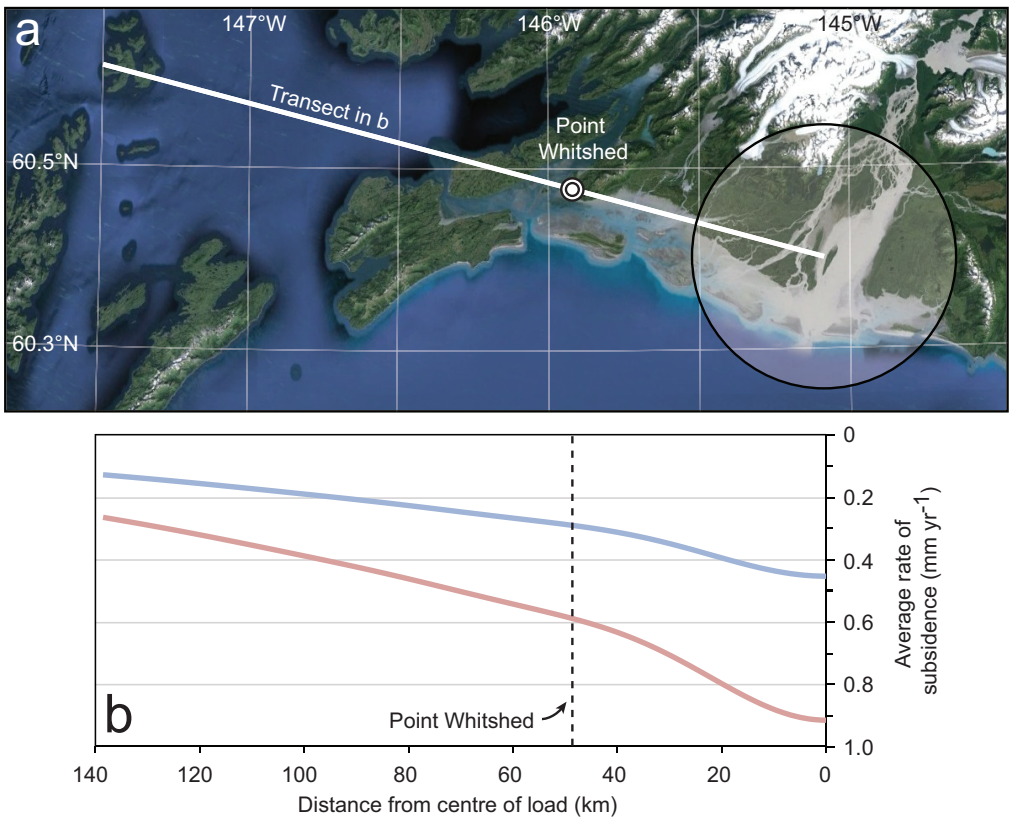

Figure 9: In (a) we model the sediment load from the Copper River Delta as a 50 km diameter disc to derive subsidence estimates for a transect through Point Whitshed. Holocene average subsidence rates in (b) are derived from linear loading histories reflecting annual sediment deposition of either 70 x 10^6 t yr^{-1} (blue) or 140 x 10^6 t yr^{-1} (red) (following Jaeger et al., 1998; Milliman and Syvistski, 1992).

Late Holocene glacial isostasy

An additional line of evidence that leads to further improvement in our model is the isolation of Lower Whitshed Lake from the sea, with the gradual beginning illustrated by marine diatoms starting to decline in abundance by AD 1850 – 1910 (section 4.1). We include a sea-level contribution from Little Ice Age and older Neoglacial changes in ice mass by adding the modelled GIA component of relative sea-level change at Cordova (Figure 6b), to RSL_4 to derive RSL_5 in Figure 10. With the addition of this contribution, we get a clear expression of relative sea-level fall commencing before 1964 (RSL_5 in Figure 10).

With the addition of recent ice loading, the total influence of sediment loading and sediment compaction required to fit the Copper River Delta observations decreases to ~1.2 mm yr^{-1} (RSL_6 in Figure 10). RSL_6 therefore incorporates RSL_2, the sea-level response to recent changes in ice mass and a combined influence of sediment loading and compaction equal to 1.2 mm yr^{-1}. The sediment load model (Figure 9) suggests loading may account for half of this amount (0.47 to 0.93 mm yr^{-1}), implying the contributions of loading and compaction to relative sea-level change may be approximately equal in magnitude.

Had we a better constraint on the elevation of Lower Whitshed Lake and evidence from other low-lying lakes in the area, we could also start to consider the different contributions of sediment loading, sediment compaction, GIA and tectonics to relative sea-level fall over the last century. The combination of just one isolation basin and the Copper River Delta evidence is a good start and shows the potential for new avenues of research.

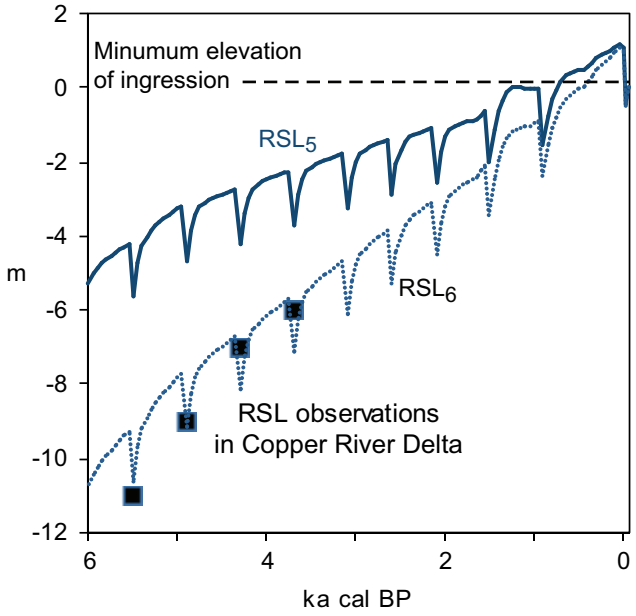

Figure 10: We define a sea-level contribution from Neoglacial and Little Ice Age changes in mass balance (GIA_{LIA}; Figure 6b and Barlow et al., 2012) and add this to RSL_4 (Figure 8) to derive a prediction (RSL_5) for Lower Whitshed Lake, where there is no contribution from sediment compaction. This satisfactorily fits the observed relative sea-level change at Lower Whitshed Lake. The elevation of the sill is uncertain and the elevation used here is just one possibility from a range of values. With the addition of the GIA_{LIA} contribution, a combined influence of ~1.2 mm yr^{-1} from sediment loading and compaction is sufficient to fit the RSL observations from Copper River Delta (RSL_6), reduced from ~1.5 mm yr^{-1} used in RSL_3 (Figure 8).

6. Conclusions

Contrasting records of environmental change from lake basins and submerged deltaic wetland environments provide constraints on the magnitudes of a range of Earth system processes through their expression in relative sea-level change. Basal sediment ages from Upper Whitshed Lake indicate ice-free conditions by at least 14,140-15,040 cal yr BP, following a Last Glacial Maximum ice extent out to the shelf edge. Both Upper and Lower Whitshed Lakes, ~33 and 4 m MSL respectively, only provide upper limits to relative sea-level change, so the rapid sea-level fall seen in other deglaciated regions remains poorly constrained in south central Alaska. Interbedded layers of freshwater peat and intertidal silt extending more than 11 m below present high tide at Copper River Delta indicate net submergence over the last 6000 years and multiple earthquake deformation cycles. In contrast, Lower Whitshed Lake records only one episode of marine sedimentation, commencing AD 1120 – 1500, that we interpret as the result of isostatic subsidence due to

Little Ice Age mass accumulation of the Chugach Mountain glaciers. Lower Whitshed Lake also records isostatic uplift at the end of the Little Ice Age before the end of marine sedimentation caused by ~1.5 m coseismic uplift in the great Alaska earthquake of 1964.

We use a model to illustrate the interaction of eustatic sea-level rise, glacial isostasy, earthquake deformation cycles, sediment loading, sediment compaction and late Holocene changes in glacier mass balance. The key drivers and constraints are:

- eustasy, for which we take a reasonable mid range estimate (Bradley et al., 2008, 2011);
- post-Last Glacial Maximum GIA with most recovery complete by the early Holocene, as reported for comparable plate boundary locations (e.g. Hutchinson et al. 2004; James et al., 2000);
- Neoglacial earth and ice model parameters previously reported for the region (Barlow et al., 2012; Larsen et al., 2005);
- a simple EDC model within the range of published values, with deformation similar to AD 1964 (Plafker, 1969) and a recurrence pattern established from regional correlations (Carver and Plafker, 2008; Shennan et al., 2014);
- the sill elevation of Lower Whitshed Lake, estimated as 1.13 ± 1 m;
- spatially variable subsidence from sediment loading predicted by a model with reasonable parameters for earth properties (Barlow et al., 2012; Larsen et al., 2005) and a simple estimate of the Holocene sediment load (Jaeger et al., 1998; Milliman and Syvistski, 1992);
- a reasonable estimate of the net effect of sediment compaction, within the ranges derived in other areas.

In combining these parameters, our model successfully explains the records of sea-level change obtained from the Whitshed Lakes and Copper River Delta. To improve further on the initial constraints on the individual contribution of these processes, we require a larger number of well dated late Holocene isolation basins at precisely constrained elevations, additional information on the height of the Last Glacial Maximum marine limit and further comparisons with tide gauge and GPS data. We suggest that isolation basin methods, incorporating the marine record from lakes now above present sea level, are a currently under-used research resource in improving our understanding of a wide range of processes that interlink in the highly dynamic region that is coastal south central Alaska.

Acknowledgements

Scott Anderson, Hannah Bailey, Katie Detrich and Joe Licciardi assisted in the field, and Scott Anderson, Katherine Cooper, Michael Ketterer and John Southon provided supporting laboratory analysis. Fieldwork and geochronology was funded by the US National Science Foundation (EAR-0823522 and ARC-0909332). Eyak Corporation kindly allowed access to their land. The modelling was developed through U.S. Geological Survey, Department of the Interior, earthquake hazards projects awards G09AP00105, G12AP20084 and G13AP00051 (the views and conclusions contained in this document are those of the authors and should not be interpreted as necessarily representing the official policies, either expressed or implied, of the U.S. Government). We thank Thomas James and an anonymous reviewer for their constructive comments and Jeff Freymueller for his editorial input, which has greatly improved this manuscript. This paper is a contribution to IGCP project 588 "Preparing for coastal change: A detailed process–response framework for coastal change at different timescales" and we thank participants of the IGCP 588 5th Annual Meeting, Cordova, Alaska, 2014 for their comments on this work.

References

Anderson, D.L., 1975. Accelerated plate tectonics. Science 187, 1077-1079.

Arendt, A.A., Eschelmeyer, K.A., Harrison, W.D., Lingle, C.S., Valentine, V.B., 2002. Rapid wastage of Alaska glaciers and their contribution to rising sea level. Science 297, 382–386.

Barclay, D.J., Wiles, G.C., Calkin, P.E., 2009. Holocene glacier fluctations in Alaska. Quaternary Science Reviews 28, 2034-2048.

Barclay, D.J., Yager, E.M., graves, J., Kloczko, M., Calkin, P.E., 2013. Late Holocene glacial history of the Copper River Delta, coastal south-central Alaska, and controls on valley glacier fluctuations. Quaternary Science Reviews 81, 74-89.

Barlow, N.L.M., Shennan, I., Long, A.J., 2012. Relative sea-level response to Little Ice Age ice mass change in south central Alaska: Reconciling model predictions and geological evidence. Earth and Planetary Science Letters 315, 62-75.

Bentley, M.J., Hodgson, D.A., Smith, J.A., Cox, N.J., 2005. Relative sea level curves for the South Shetland Islands and Marguerite Bay, Antarctic peninsula. Quaternary Science Reviews 24, 1203-1216.

Berthier, E., Schiefer, E., Clarke, G.K.C., Menounos, B., Remy, F., 2010. Contribution of Alaskan glaciers to sea-level rise derived from satellite imagery. Nature Geoscience 3, 92-95.

Blaauw, M., Christen, J.A., 2011. Flexible paleoclimate age-depth models using an autoregressive gamma process. Bayesian Analysis 6, 457-474.

Bradley, S.L., Milne, G.A., Shennan, I., Edwards, R., 2011. An improved glacial isostatic adjustment model for the British Isles. Journal of Quaternary Scince 26, 541–552.

Bradley, S.L., Milne, G.A., Zong, Y., Horton, B., 2008. Modelling sea-level data from China and Malay-Thai Peninsula to infer Holocene eustatic sea-level change. American Geophysical Union, Fall Meeting 2008. Abstract #GC33A-0763.

Bronk Ramsey, C., 2009. Bayesian analysis of radiocarbon dates. Radiocarbon 51(1), 337-360.

Calkin, P.E., 1988. Holocene glaciation of Alaska (and adjoining Yukon Territory, Canada). Quaternary Science Reviews 7, 159–184.

Calkin, P.E., Wiles, G.C., Barclay, D.J., 2001. Holocene coastal glaciation of Alaska. Quaternary Science Reviews 20, 449–461.

Carlson, P.R., Molnia, B.F., 1975. Preliminary isopach map of Holocene sediments, northern Gulf of Alaska. United States Geological Survey Open File Map 75-507.

Carver, G., Plafker, G. 2008. Paleoseismicity and Neotectonics of the Aleutian Subduction Zone—An Overview, in Active Tectonics and Seismic Potential of Alaska, AGU Geophysical Monograph, 179, J.T. Freymueller, P.J. Haeussler, R. Wesson, and G. Ekstrom, eds., AGU, Washington, D.C.

Clague, J., Harper, J.R., Hebda, R.J., Howes, D.E., 1982. Late Quaternary sea levels and crustal movements, coastal British Columbia. Canadian Journal of Earth Sciences 19, 597–618

Enkelmann, E., Garver, J. I., Pavlis, T. L. 2008. Rapid exhumation of ice-covered rocks of the Chugach–St. Elias orogen, Southeast Alaska. Geology 36, 915-918.

Fuis, G.S., Moore, T.E., Plafker, G., Brocher, T.M., Fisher, M.A., Mooney, W.D., Nokleberg, W.J., Page, R.A., Beaudoin, B.C., Christensen, N.I., Levander, A.R., Lutter, W.J., Saltus, R.W., Ruppert, N.A., 2008. Trans-Alaska Crustal Transect and continental evolution involving subduction underplating and synchronous foreland thrusting: Geology, 36, p. 267–270, doi: 10.1130/G24257A.1.

Hafsten, U., Tallantire, P.A., 1978. Palaeoecology and post-Weichselian shore-level changes on the coast of Møre, western Norway. Boreas *7*, 109–122.

Hamilton, T.D., Thorson, R.M., 1983. The Cordilleran Ice Sheet in Alaska. In: Porter, S.C. (Ed.), The Late Pleistocene. Late Quaternary environments of the United States, vol. 1. University of Minnesota Press, Minneapolis, pp. 38–52.

Hartley, B., Barber, H.G., Carter, J.R., 1996. An Atlas of British Diatoms. Biopress, Bristol.

Hemphill-Haley, E., 1993. Taxonomy of recent and fossil (Holocene) diatoms (Bacilloriophyta) from northern Willapa Bay, Washington. US Geological Survey Open File Report 93-289, 1-151.

Heusser, C.J., 1960, Late Pleistocene environments of North Pacific North America. American Geographical Society Special Publication, v. 35

Horton, B.P., Shennan, I., 2009. Compaction of Holocene strata and the implications for relative sea- level change on the east coast of England. Geology 37, 1083-1086.

Hutchinson, I., James, T.S., Clague, J.J., Barrie, W., Conway, K.W., 2004. Reconstruction of late Quaternary sea-level change in southwestern British Columbia from sediments in isolation basins. Boreas 33, 183-194.

Ingólfsson, Ó., Norðdahl, H., Hafliðason, H., 1995. Rapid isostatic rebound in southwestern Iceland at the end of the last deglaciation. Boreas 24, 245-259.

Jaeger, J.M., Nittrouer, C.A., Scott, N.D., Milliman, J.D., 1998. Sediment accumulation along a glacially impacted mountainous coastline: north-east Gulf of Alaska. Basin Research 10, 155-173.

James, T.S., Clague, J.J., Wang, K., Hutchinson, I., 2000. Postglacial rebound at the northern Cascadia subduction zone. Quaternary Science Reviews 19, 1527-1541.

James, T.S., Gowan, E.J., Hutchinson, I., Clague, J.J., Barrie, J.V., Conway, K.W., 2009a. Sea-level change and paleogeographic reconstructions, southern Vancouver Island, British Columbia, Canada. Quaternary Science Reviews 28, 1200-1216.

James, T. S., Gowan, E. J., Wada, I., Wang, K. 2009b. Viscosity of the asthenosphere from glacial isostatic adjustment and subduction dynamics at the northern Cascadia subduction zone, British Columbia, Canada. Journal of Geophysical Research: Solid Earth 114, B04405.

James, T.S., Hutchinson, I., Barrie, V.B., Conway, K.W., 2005. Relative Sea-level Change in the northern Strait of Georgia, British Columbia. Geographie Physique et Quaternaire 59, 113-127.

Josenhans, H.W., Fedje, D.W., Conway, K.W., Barrie, J.V., 1995. Post glacial sea levels on the western Canadian continental shelf: evidence for rapid change, extensive subaerial exposure, and early human habitation. Marine Geology 125, 73–94.

Kaufman, D.S., Manley, W.F., 2004. Pleistocene maximum and Late Wisconsinan glacier extents across Alaska, U.S.A. In: Ehlers, J., Gibbard, P.L. (Eds.), Quaternary Glaciations – Extent and Chronology, Part II: North America. Developments in Quaternary Science, vol. 2B. Elsevier, Amsterdam, pp. 9–27

Ketterer, M.E., Hafer, K.M., Jones, V.J., Appleby, P.G., 2004. Rapid dating of recent sediments in Loch Ness: inductively coupled plasma mass spectrometric measurements of global fallout plutonium. Science of the Total Environment 322, 221–229.

Krzywinski, K., Stabell, B., 1984. Late Weichselian sea level changes at Sotra, Hordaland, western Norway. Boreas 13, 159–202.

Larsen, C.F., Motyka, R.J., Arendt, A.A., Echelmeyer, K.A., Geissler, P.E., 2007. Glacier changes in southeast Alaska and northwest British Columbia and contribution to sea level rise. Journal of Geophysical Research 112, F01007. doi:10.1029/2006JF000586.

Larsen, C.F., Motyka, R.J., Freymueller, J.T., Echelmeyer, K.A., Ivins, E.R., 2004. Rapid uplift of southern Alaska caused by recent ice loss. Geophysical Journal International 158, 1118-1133.

Larsen, C.F., Motyka, R.J., Freymueller, J.T., Echelmeyer, K.A., Ivins, E.R., 2005. Rapid viscoelastic uplift in southeast Alaska caused by post-Little Ice Age glacial retreat. Earth And Planetary Science Letters 237, 548-560.

Lloyd, J.M., Norddahl, H., Bentley, M.J., Newton, A.J., Tucker, O., Zong, Y., 2009. Lateglacial to Holocene relative sea-level changes in the Bjarkarlundur area near Reykholar, North West Iceland. Journal of Quaternary Science 24, 816-831.

Long, A.J., Woodroffe, S.A., Roberts, D.H., Dawson, S. 2011. Isolation basins, sea-level changes and the Holocene history of the Greenland Ice Sheet. Quaternary Science Reviews 30, 3748-3768.

Mann, D.H., Hamilton, T.D., 1995. Late Pleistocene and Holocene palaeoenvironments of the north Pacific coast. Quaternary Science Reviews 14, 449-471.

McKay, N.P., Kaufman, D.S., 2009. Holocene climate and glacier variability at Hallet and Greyling Lakes, Chugach Mountains, south-central Alaska. Journal of Paleolimnology 41, 143–159.

Milliman, J. D., Syvitski, J. P. 1992. Geomorphic/tectonic control of sediment discharge to the ocean: the importance of small mountainous rivers.The Journal of Geology, 100, 525-544.

Molnia, B.F., 2008. Glaciers of North America – Glaciers of Alaska. In: Williams, R.S., Jr. and Ferrigno, J.G., (Eds.), Satellite image atlas of glaciers of the world. U.S. Geological Survey Professional Paper 1386-K, 525 pp.

Molnia, B.F., Post, A., 1995. Holocene history of Bering Glacier, Alaska: a prelude to the 1993-1994 surge. Physical Geography 16, 87-117.

National Oceanic and Atmospheric Administration (NOAA), 2014. Cordova Mean Sea Level Trend. Available at http://tidesandcurrents.noaa.gov. Accessed 25th May 2014.

Palmer, A.J.M., Abbott, W.H., 1986. Diatoms as indicators of sea-level change. In van de Plassche, O. (editor), Sea-level research. Free University, 457-87.

Pasch, A. D., Foster, N. R., Irvine, G. V. 2010. Faunal analysis of late Pleistocene–early Holocene invertebrates provides evidence for paleoenvironments of a Gulf of Alaska shoreline inland of the present Bering Glacier margin. Geological Society of America Special Papers, 462, 251-274.

Patrick, R., Reimer, C.W., 1966. The Diatoms of the United States. Volume 1. Monographs of The Academy of Natural Sciences of Philadelphia No 13. Academy of Natural Sciences of Philadelphia, Philadelphia.

Patrick, R., Reimer, C.W., 1975. The Diatoms of the United States. Volume 2, Part 1. Monographs of The Academy of Natural Sciences of Philadelphia No 13. The Academy of Natural Sciences of Philadelphia, Philadelphia.

Plafker, G., 1969. Tectonics of the March 27, 1964 Alaska earthquake: U.S. Geological Survey Professional Paper 543–I, 74 p., 2 sheets, scales 1:2,000,000 and 1:500,000, http://pubs.usgs.gov/pp/0543i/.

Plafker, G., Lajoie, K.R., Rubin, M., 1992. Determining intervals of great subduction zone earthquakes in southern Alaska by radiocarbon dating. In: Taylor, R.E., Long, A., Kra, R.S. (Eds.), Radiocarbon after Four Decades. An Interdisciplinary Perspective. Springer Verlag, New York, pp. 436-452.

Reger, R.D., 1991. Deglaciation of the Allison-Sawmill Creeks area, southern shore of Port Valdez, Alaska, In: Reger, R.D. (Ed.), Short Notes on Alaskan Geology. Alaska Division of Geological and Geophysical Surveys Professional Report 111G, pp. 55-61.

Reimer, P.J., Bard, E., Bayliss, A., Beck, J.W., Blackwell, P.G., Bronk Ramsey, C., Buck, C.E., Edwards, R.L., Friedrich, M., Grootes, P.M., Guilderson, T.P., Haflidason, H., Hajdas, I., Hatté, C., Heaton, T.J., Hoffmann, D.L., Hogg, A.G., Hughen, K.A., Kaiser, K.F., Kromer, B., Manning, S.W., Niu, M., Reimer, R.W., Richards, D.A., Scott, M.E., Southon, J.R., Turney, C.S.M., van der Plicht, J., 2013. IntCal13 and Marine13

radiocarbon age calibration curves 0-50,000 yr cal BP. Radiocarbon 55 (4), 1869-1887.

Reyes, A.V., Wiles, G.C., Smith, D.J., Barclay, D.J., Allen, S., Jackson, S., Laxton, S., Lewis, D., Calkin, P.E., Clague, J., 2006. Expansion of alpine glaciers in Pacific North America in the first millennium A.D. Geology 34, 57-60.

Rundgren, M., Ingólfsson, Ó., Björk, S., Haflidason, H., 1997. Dynamic sea-level change during the last deglaciation in northern Iceland. Boreas 26, 201–215.

Sauber, J., Plafker, G., Molnia, B. F., Bryant, M. A. 2000. Crustal deformation associated with glacial fluctuations in the eastern Chugach Mountains, Alaska. Journal of Geophysical Research: Solid Earth (1978–2012),105, 8055-8077.

Shennan, I., Bruhn, R., Barlow, N., Good, K., Hocking, E., 2014. Late Holocene great earthquakes in the eastern part of the Aleutian megathrust. Quaternary Science Reviews 84, 86-97.

Shennan, I., Bruhn, R., Plafker, G., 2009. Multi-segment earthquakes and tsunami potential of the Aleutian megathrust. Quaternary Science Reviews 28, 7-13

Shennan, I., Innes, J.B., Long, A.J., Zong, Y., 1994. Late Devensian and Holocene relative sea-level changes at Loch nan Eala, near Arisaig, Northwest Scotland. Journal of Quaternary Science 9, 261-283.

Shennan, I., Innes, J. B., Long, A. J., Zong, Y., 1995. Late Devensian and Holocene relative sea-level changes in northwestern Scotland: new data to test existing models. Quaternary International 26, 97–123.

Sirkin, L.T., Tuthill, S.J., 1987. Late Pleistocene and Holocene deglaciation and environments of the southern Chugach Mountains, Alaska. Geological Society of America Bulletin 99, 376-384.

Spada, G., 2003. The Theory Behind TABOO. Samizdat Press, Golden-White River Junction.

Spada, G., Antonioli, A., Boschi, L., Brandi, V., Cianetti, S., Galvani, G., Giunchi, C., Perniola, B., Piana Agostinetti, N., Piersanti, A., Stocchi, P., 2003. TABOO, User Guide. Samizdat Press, Golden-White River Junction.

Spada, G., Antonioli, A., Boschi, L., Brandi, V., Cianetti, S., Galvani, G., Giunchi, C., Perniola, B., Piana Agostinetti, N., Piersanti, A., Stocchi, P., 2004. Geodesy: modeling earth's post-glacial rebound. Eos Transactions AGU 85, 62.

Svendsen, J.J., Mangerud, J., 1987. Late Weichselian and Holocene sea level history for a cross-section of western Norway. Journal of Quaternary Science 2, 113-132.

Törnqvist, T.E., Wallace, D.J., Storms, J.E.A., Wallinga, J., van Dam, R.L., Blaauw, M., Derksen, M.S., Klerks, C.J.W., Meijneken, C., Snijders, E.M.A., 2008. Mississippi Delta subsidence primarily caused by compaction of Holocene strata. Nature Geoscience, 1, 173–176.

van der Werff, A., Huls, H., 1958-1974. Diatomeeenflora van Nederland. 8 parts. Published privately, De Hoef, The Netherlands.

Vos, P.C., de Wolf, H., 1988. Methodological aspects of palaeo-ecological diatom research in coastal areas of the Netherlands. Geologie en Mijnbouw 67, 31-40.

Wiles, G.C., Barclay, D.J., Calkin, P.E., 1999. Tree-ring-dated Little Ice Age histories of maritime glaciers from western Prince William Sound, Alaska. The Holocene 9, 163–173.

Wiles, G.C., Barclay, D.J., Calkin, P.E., Lowell, T.V., 2008. Century to millennial-scale temperature variations for the last two thousand years inferred from glacial geologic records of southern Alaska. Global and Planetary Change 60, 115–125. doi:10.1016/j.gloplacha.2006.07.036.

Wiles, G.C., Calkin, P.E., 1994. Late Holocene, high-resolution glacial chronologies and climate, Kenai Mountains, Alaska. Geological Society of America Bulletin 106, 281–303.

Yu, S.-Y., Törnqvist, T.E., Hu, P., 2012. Quantifying Holocene lithospheric subsidence rates underneath the Mississippi Delta. Earth and Planetary Science Letters 331-332, 21-30.

Yu, Z., Walker, K.N., Evenson, E.B., Hajdas, I., 2008. Lateglacial and early Holocene climate oscillations in the Matanuska Valley, south-central Alaska. Quaternary Science Reviews 27, 148-161.

Zander, P.D., Kaufman, D.S., Kuehn, S.C., Wallace, K.L., Anderson, R.S., 2013. Early and late Holocene glacial fluctuations and tephrostratigraphy, Cabin Lake, Alaska. Journal of Quaternary Science 28, 761-771.

Zwartz, D., Bird, M., Stone, M., Lambeck, K., 1998. Holocene sea level change and ice-sheet history in the Vestfold Hills, East Antarctica. Earth and Planetary Science Letters 155, 131-145.

Supplementary info

Table S1: Plutonium in core 10-WS-1A, Lower Whitshed

Table S2: Diatom species lists for samples from core 11-UW-2-3, Upper Whitshed